10.1109/ULTSYM.2012.0533

Effects of Masks on Reconstruction of High-Frame-Rate Images

Jian-yu Lu
Ultrasound Lab, Department of Bioengineering, The University of Toledo
Toledo, OH 43606, USA
Email: jilu@eng.utoledo.edu

***Abstract* – A set of strip masks have been developed for high frame rate imaging with steered plane wave (SPW), steered diverging beam (SDB), and limited-diffraction beam (LDB) transmissions. These masks enhance image contrasts significantly. In addition, an image mask was developed for reconstructed images. The mask allows the reconstructed images to have a similar brightness within their fields of views.**

Keywords - ***High-frame-rate imaging, masks, fast Fourier transform, limited-diffraction beams, and diverging beams***

I. Introduction

High-frame-rate (HFR) imaging method based on limited-diffraction beam theory for pulse-echo imaging has been studied extensively [1]-[20]. The method has the advantages of high resolution, high contrast, large field of view, and a good resistance to phase aberration and noise as compared to the conventional line-by-line delay-and-sum (D&S) imaging using the same number of transmissions [1]-[4]. However, because the HFR imaging method reconstructs one strip of image from each transmission using the fast Fourier transform, digital noise may be produced outside the strip illuminated by transmission beams such as steered plane wave (SPW) [3]-[4], steered diverging beam (SDB) [5]-[6], and limited-diffraction beam (LDB) [1]-[4]. To reduce the noise and thus enhance image contrast, a mask is needed for each image strip before the image strips are coherently or incoherently superposed to form a final image of a high quality and large field of view. In addition, another mask that provides both angular and axial compensations is needed to ensure that the final images have a similar brightness in the entire image field of view.

II. Masks

A. *Strip Mask for Steered Plane Wave and Steered Diverging Beam Transmissions*

A strip mask is designed so that the transitions between strip images are smooth along the both axial and angular directions (see Figs. 2(a)-2(d)). The strip mask $m_s(x,z)$ for both the steered plane wave (SPW) [3]-[4] and the steered diverging beam (SDB) [5] transmissions is given by:

$$m_s(x,z)=\begin{cases}1-(\phi_1-\alpha_z)/\alpha_t, & -x_{zt}^{'}\le x'<-x_z^{'}\\ f(x,z)+1, & -x_z^{'}\le x'\le x_z^{'}\\ 1-(\phi_2-\alpha_z)/\alpha_t, & x_z^{'}<x'\le x_{zt}^{'}\\ 0, & \text{otherwise}\end{cases}, \quad (1)$$

where

$$\phi_1=\left|\tan^{-1}\frac{x'+(D/2)\cos\zeta}{z'}\right|, \quad (2)$$

$$\phi_2=\left|\tan^{-1}\frac{x'-(D/2)\cos\zeta}{z'}\right|, \quad (3)$$

and where D is the aperture of the array, ζ is the steering angle of SPW or SDB, $\alpha\ge 0$ is the diverging angle of SDB, and the coordinates (x',z') are rotated by a steering angle ζ from the coordinates (x,z) as shown in Fig. 1:

$$\begin{cases}x'=x\cos\zeta+z\sin\zeta\\ z'=-x\sin\zeta+z\cos\zeta\end{cases}, \quad (4)$$

and where

$$x_{zt}^{'}=z'\tan\alpha_{zt}+\frac{D}{2}\cos\zeta \quad (5)$$

and

$$x_z^{'}=z'\tan\alpha_z+\frac{D}{2}\cos\zeta \quad (6)$$

are the boundary of the strip mask and the boundary that is determined by the diverging angle, respectively, where $\alpha_{zt}=\alpha_z+\alpha_t$, and

$$\alpha_z=\begin{cases}\left|\frac{\alpha}{2}\left(\frac{z'}{z_t}\right)^{1+(180\alpha/\pi-6)/6}\right|, & z'\le z_t\\ \left|\frac{\alpha}{2}\right|, & z'>z_t\end{cases} \quad (7)$$

and

$$\alpha_t = \frac{\zeta_s}{N-1}, \tag{8}$$

and where $z_t = 120$ mm is a preset transition distance, $\zeta_s \geq 0$ (90^o in this paper) is the sector angle that determines the field of view of images, and $N > 1$ is the number of transmissions to form a final image.

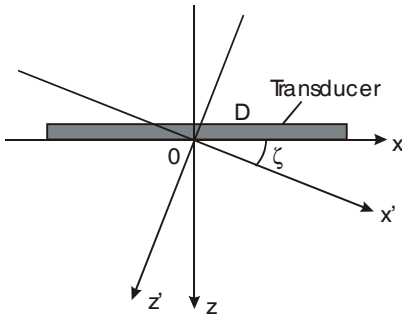

Figure 1. Rotation of coordinates from (x, z) to (x', z') by a steering angle ζ.

The angular compensation within the area determined by the diverging angle is given by the following cosine function:

$$f(x,z) = \begin{cases} A_\alpha \cos^{1+\frac{180\alpha}{15\pi}} \phi_\alpha, & z' \leq z_t \\ A_\alpha \cos^{0.1+0.9\left(1-\frac{z'-z_t}{z_c}\right)+\frac{180\alpha}{15\pi}} \phi_\alpha, & z_t < z' \leq z_{tc} \\ A_\alpha \cos^{0.1+\frac{180\alpha}{15\pi}} \phi_\alpha, & z' > z_{tc} \end{cases}, \tag{9}$$

where

$$A_\alpha = \frac{180\alpha}{3\pi}\left(1+\frac{180\alpha}{5\pi}\right) \tag{10}$$

and

$$\phi_\alpha = \frac{\pi x'}{2x_z'} \tag{11}$$

are the amplitude and phase of the cosine function respectively, $z_{tc} = z_t + z_c$, and $z_c = 10$ mm is a preset transition radius.

B. *Strip Mask for Limited-Diffraction Beam Transmission*

For limited-diffraction beam (LDB) transmission, the LDB aperture weighting needs to be converted to a corresponding steering angle. The relationship between the equivalent steering angle ζ_c and LDB transmit aperture weighting parameter k_{x_T} at the center wave number k_c is given by:

$$\zeta_c = \sin^{-1}\frac{k_{x_T}}{k_c} = \sin^{-1}\frac{k_{x_T} c}{2\pi f_c}, \tag{12}$$

where $k_c = 2\pi f_c / c$, f_c is the center frequency, and c is the speed of sound.

Since in medical imaging, broadband transducers are used to achieve a high axial resolution, the steering angle has a range, i.e., $\zeta_l \leq \zeta \leq \zeta_h$, where $\zeta_l = \sin^{-1}\left[k_{x_T} c/(2\pi f_l)\right]$ and $\zeta_h = \sin^{-1}\left[k_{x_T} c/(2\pi f_h)\right]$, and where f_l and f_h are the low and high ends of the -6dB pass band of the transmit beam of the transducer.

Based on the relationship of the equivalent steering angles above, a strip mask is developed for LDB transmission as follows (see Figs. 2(e)-2(f)):

$$m_{s_{LDB}}(x,z) = \begin{cases} \sin^{p_0}\left(\frac{\pi}{2}\frac{x-x_l}{x_c-x_l}\right), & x_l \leq x \leq x_c \\ \sin^{p_0}\left(\frac{\pi}{2}\frac{x_h-x}{x_h-x_c}\right), & x_c < x \leq x_h \\ 0, & \text{otherwise} \end{cases}, \tag{13}$$

where

$$x_l = \begin{cases} z\tan\zeta_l - \gamma D, & k_{x_T} \geq 0 \\ z\tan\zeta_h - \gamma D, & k_{x_T} < 0 \end{cases} \tag{14}$$

and

$$x_h = \begin{cases} z\tan\zeta_h + \gamma D, & k_{x_T} \geq 0 \\ z\tan\zeta_l + \gamma D, & k_{x_T} < 0 \end{cases}, \tag{15}$$

and $x_c = z\tan\zeta_c$ and $z > 0$, and where $p_0 = 1$ and $\gamma = 1$ in this study.

C. *Image Mask for Axial and Angular Compensations*

The HFR imaging theory assumes that both transmit and receive beams are produced with an infinite aperture. However, any practical transducers always have a finite aperture. Therefore, a mask that provides both axial and angular amplitude compensations for reconstructed images is needed (see Fig. 3). In the HFR imaging method, strips of images obtained from individual transmissions can be coherently superposed to form a high quality final image. Since the widths of the strips are finite, they are superposed multiple times near the surface of transducers but are superposed fewer number of times at a larger depth. In addition, as the steering angle increases, the image strips become thinner and thus images may appear darker. Therefore, an image mask $m_i(x,z)$ is created to increase the "gain" at both larger depths and steering angles:

$$m_i(x,z)=\begin{cases} g(r_1)+1, & |\phi|\le\phi_0 \\ g(r_1)q(\phi)+1, & \phi_0<|\phi|\le\zeta_s/2, \\ 0, & \text{elsewhere} \end{cases} \quad (16)$$

where

$$g(r_1)=\left(\frac{r_1-z_a}{\Delta_r}\right)^{p_1} \quad (17)$$

and

$$q(\phi)=1+(A_q-1)\left(\frac{|\phi|-\phi_0}{\zeta_s/2-\phi_0}\right)^{p_2}, \quad (18)$$

and where $r_1=\sqrt{x^2+(z+z_a)^2}\le r_d+z_a$, $z_a=(D/2)\cot(\zeta_s/2)\ge 0$ is the position of the apex that is behind the transducer, r_d is the maximum depth of the image, $\phi=\tan^{-1}[x/(z+z_a)]$ with $|x|\le z\tan(\zeta_s/2)+D/2$, Δ_r=0.3 mm, p_1=1, p_2=2, A_q=2, and $\phi_0=20^o$.

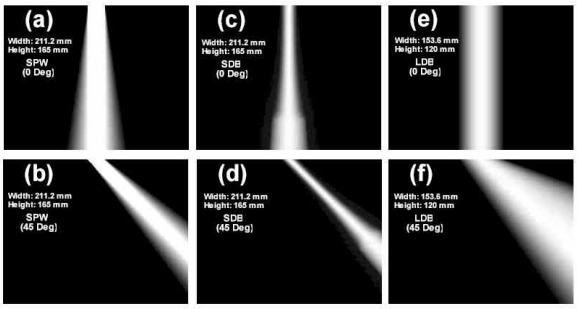

Figure 2. Strip masks for SPW, SDB (9 degree divergence), and LDB at both 0 (top row) and 45 degrees (botom row). The masks are normalized to the brightest point.

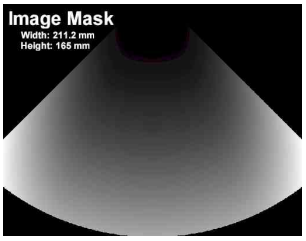

Figure 3. Image mask with both angular and axial amplitude compensations. The mask is normalized to the brightest point.

III. Experiment

An experiment was performed to show the effects of the masks developed above on the contrast of reconstructed images. In the experiment, radio-frequency (RF) echo signals were acquired with a home-made HFR imaging system for image reconstructions. A 128-element, 19.2-mm aperture, and 2.5-MHz linear array transducer of about 58% -6-dB pulse-echo fractional bandwidth was used. An ATS539 phantom (ATS, Connecticut, USA) was used as a test object (Fig. 4). 11 (Fig. 5) and 91 (Fig. 6) transmissions respectively were used to obtain a final coherently superposed image of more than 90-degree field of view (about 486 and 325 frames/s for image depths of 120 and 180 mm respectively for 11 transmissions and about 58 and 39 frames/s for image depths of 120 and 180 mm respectively for 91 transmissions). Strip masks (Fig. 2) in addition to the angular and axial amplitude compensation mask (Fig. 3) were applied to the HFR images reconstructed with SPW, SDB (9 degrees), and LDB transmissions respectively (see Figs. 5 and 6). Notice that only 165 out of 180 mm of the image depth are displayed in the figure.

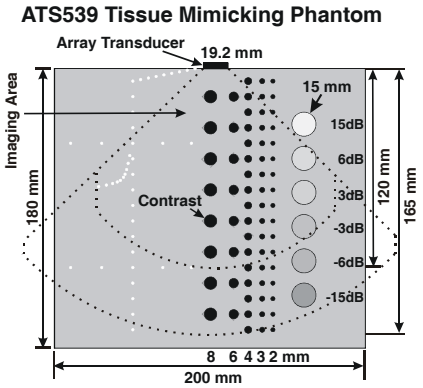

Figure 4. A cross-section of an ATS539 tissue-mimicking phantom showing the imaging areas of 120 mm and 165 mm depths with +/-45 degree field of view for the experiments. (Modified from Fig. 2 of the 2011 IEEE IUS diverging beam paper [5].)

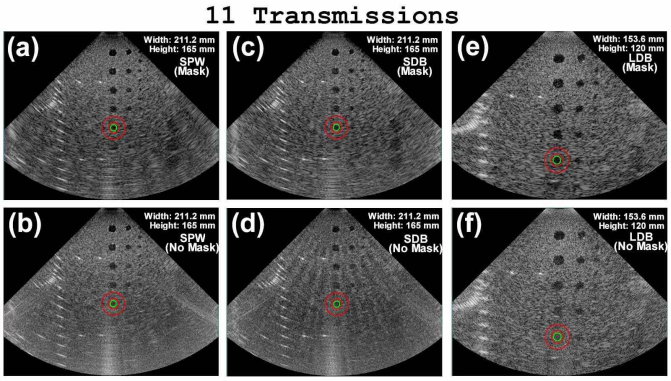

Figure 5. Effects of masks on images reconstructed with the HFR imaging method with 11 transmissions. 50 dB log compression has been applied.

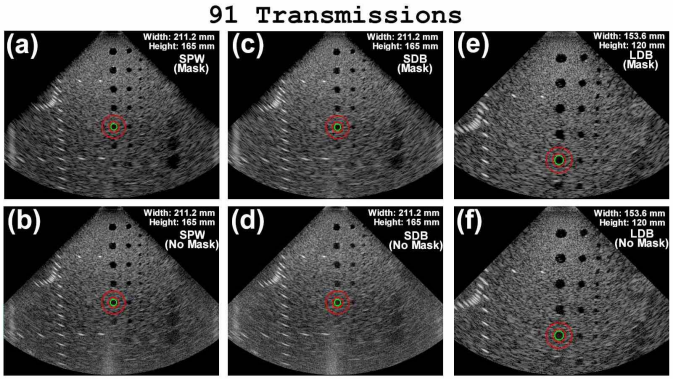

Figure 6. Effects of masks on images reconstructed with the HFR imaging method with 91 transmissions. 50 dB log compression has been applied..

IV. Results

Table I shows that for 11 transmissions (Fig. 5), contrasts (i.e., 20 times the base-10 logarithm of the ratio between the mean pixel values of the green inner circle and outer red rings) of a cyst (Fig. 4) of the ATS539 tissue-mimicking phantom are increased from -4.98 to -9.08, -4.32 to -7.23, and -3.34 to -8.82 dB, respectively, for images reconstructed with SPW ((a) and (b)), 9-degree divergence SDB ((c) and (d)), and LDB ((e) and (f)) transmissions after applying the strip masks. For 91 transmissions (Fig. 6), corresponding contrasts are increased from -10.8 to -14.0, -7.32 to -11.2, and -10.4 to -14.4, respectively. (The images with and without strip masks are in the first and second rows respectively in the figures. The same angular and axial compensation mask has been applied to all images.) It is clear that images with strip masks have much higher contrasts and fewer artifacts than those without.

Table 1. Changes of contrasts of the 5th large cyst (8 mm diameter) from the top of the ATS539 tissue-mimicking phantom due to strip masks.

Cyst Contrast (dB)	11 Transmissions		91 Transmissions	
	No Strip Mask	Strip Mask	No Strip Mask	Strip Mask
SPW	-4.98	-9.08	-10.80	-14.03
SDB (9^o)	-4.32	-7.23	-7.32	-11.26
LDB	-3.34	-8.82	-10.44	-14.42

V. Conclusion

The strip masks are essential for the high frame rate imaging method since they can improve image contrast substantially. An image mask that compensates for both angular and axial amplitudes is also necessary to ensure reconstructed images to have a similar brightness within the image field of view.

References

[1] Jian-yu Lu, "2D and 3D high frame rate imaging with limited diffraction beams," *IEEE Transactions on Ultrasonics, Ferroelectrics, and Frequency Control*, vol. 44, no. 4, pp. 839-856, July 1997.

[2] Jian-yu Lu, "Experimental study of high frame rate imaging with limited diffraction beams," *IEEE Transactions on Ultrasonics, Ferroelectrics, and Frequency Contro*l, vol. 45, no. 1, pp. 84-97, January 1998.

[3] Jiqi Cheng and Jian-yu Lu, "Extended high frame rate imaging method with limited diffraction beams," *IEEE Transactions on Ultrasonics, Ferroelectrics, and Frequency Control*, vol. 53, no. 5, pp. 880-899, May 2006.

[4] Jian-yu Lu, Jiqi Cheng, and Jing Wang, "High frame rate imaging system for limited diffraction array beam imaging with square-wave aperture weightings," *IEEE Transactions on Ultrasonics, Ferroelectrics, and Frequency Control*, vol. 53, no. 10, pp. 1796-1812, October 2006.

[5] Jian-yu Lu and Hong Chen, "High frame rate imaging with diverging beam transmission and Fourier reconstruction," in *2011 IEEE International Ultrasonics Symposium Proceedings*, pp. 2221-2224, 2011 (Digital Object Identifier: 10.1109/ULTSYM.2011.0551).

[6] Hu Peng and Jian-yu Lu, "High frame rate 2D and 3D imaging with a curved or cylindrical array," in *2002 IEEE Ultrasonics Symposium Proceedings*, 02CH37388, vol. 2, pp. 1725-1728, 2002.

[7] Jian-yu Lu, "Effects of data density of echo Fourier domain on quality of high frame rate imaging," in *2008 IEEE International Ultrasonics Symposium Proceedings*, CFP08ULT, vol. 1, pp. 974-977, 2008 (ISSN: 1051-0117) (Digital Object Identifier: 10.1109/ULTSYM.2008.0235).

[8] Jian-yu Lu and Sung-Jae Kwon, "Simplification of high frame rate imaging system with coordinate rotation," in *2007 IEEE Ultrasonics Symposium Proceedings*, 07CH37920, vol. 1, pp. 33-36, 2007 (ISSN: 1051-0117).

[9] Jing Wang and Jian-yu Lu, "Motion artifacts of extended high frame rate imaging," *IEEE Transactions on Ultrasonics, Ferroelectrics, and Frequency Control*, vol. 54, no. 7, pp. 1303-1315, July 2007.

[10] Jing Wang and Jian-yu Lu, "Effects of phase aberration and noise on extended high frame rate imaging," *Ultrasonic Imaging*, vol. 29, no. 2, pp. 105-121, April 2007.

[11] Jian-yu Lu, Zhaohui Wang, and Sung-Jae Kwon, "Blood flow velocity vector imaging with high frame rate imaging methods," in *2006 IEEE Ultrasonics Symposium Proceedings*, 06CH37777, vol. 2, pp. 963-966, 2006 (ISSN: 1051-0117).

[12] Jian-yu Lu and Jing Wang, "Square-wave aperture weightings for reception beam forming in high frame rate imaging," in *2006 IEEE Ultrasonics Symposium Proceedings*, 06CH37777, vol. 1, pp. 124-127, 2006 (ISSN: 1051-0117).

[13] Jian-yu Lu, "Ultrasonic imaging with limited diffraction beams," in the book, *Localized Waves*, Editors: Hugo E. Hernandez-Figueroa, Michel Zamboni-Rached, and Erasmo Recami, Publisher: John Wiley & Sons, Inc., New Jersey, Chapter 4, pp. 97-128, 2008 (ISBN: 978-0-470-10885-7).

[14] Jian-yu Lu and Jiqi Cheng, "Field computation for two-dimensional array transducers with limited diffraction array beams," *Ultrasonic Imaging*, vol. 27, no. 4, pp. 237-255, October 2005).

[15] Jian-yu Lu and John L. Waugaman, "Development of a linear power amplifier for high frame rate imaging system," in *2004 IEEE Ultrasonics Symposium Proceedings*, 04CH37553C, vol. 2, pp. 1413-1416, 2004 (ISSN: 1051-0117).

[16] Jian-yu Lu, Jing Wang, Hu Peng, and Jiqi Cheng, "Increasing frame rate of limited diffraction imaging system with code excitations," in *Acoustical Imaging*, vol. 26, Roman Gr. Maev, Editor, pp. 467-475, 2002 (ISBN: 0-306-47340-2).

[17] Jian-yu Lu, Jiqi Cheng, and Hu Peng, "Sidelobe reduction of images with coded limited diffraction beams," in *2001 IEEE Ultrasonics Symposium Proceedings*, 01CH37263, vol. 2, pp. 1565-1568, 2001 (ISSN: 1051-0117).

[18] Jian-yu Lu, "A study of signal-to-noise ratio of the Fourier method for construction of high frame rate images," in *Acoustical Imaging*, vol. 24, Hua Lee and G. Wade, Editors, pp. 401-406, 2000 (ISBN: 0-306-46518-3).

[19] Jian-yu Lu and Anjun Liu, "An X wave transform," *IEEE Transactions on Ultrasonics, Ferroelectrics, and Frequency Control*, vol. 47, no. 6, pp. 1472-1481, November 2000.

[20] Jian-yu Lu and Shiping He, "Effects of phase aberration on high frame rate imaging," *Ultrasound in Medicine and Biology*, vol. 26, no. 1, pp. 143-152, 2000.